Photoinduced Intramolecular Electron-Transfer Processes in [60]Fullerene and *N,N*-Bis(biphenyl)aniline Molecular Systems in Solutions

Atula S. D. Sandanayaka,[†] Kei-ichiro Ikeshita,[‡] G. Abraham Rajkumar[‡], Yoshio Furusho,[§] Yasuyuki Araki[†], Toshikazu Takata,*[,||] and Osamu Ito*[,†]

Institute of Multidisciplinary Research for Advanced Materials, Tohoku University, Katahira 2-1-1, Aoba-ku, Sendai, 980-8577, Japan, Department of Applied Chemistry, Graduated School of Engineering, Osaka Prefecture University, 1-1 Gakuen-cho, Sakai-shi, Osaka 599-8531, Japan, Yashima Super Structured Helix Project, JST, Moriyama-ku, Nagoya 552-8555, Japan, and Department of Organic and Polymeric Materials, Tokyo Institute of Technology, Ookayama, Meguro, Tokyo, 152-8552, Japan

Received: April 21, 2005; In Final Form: July 19, 2005

Photoinduced intramolecular charge-separation and charge-recombination processes in covalently connected C_{60}-(spacer)-bis(biphenyl)aniline (C_{60}-sp-BBA) and C_{60}-((spacer)-bis(biphenyl)aniline)$_2$ (C_{60}-(sp-BBA)$_2$) have been studied by time-resolved fluorescence and transient absorption methods. Since a flexible alkylthioacetoamide chain was employed as the spacer, the folded structures in which the BBA moiety approaches the C_{60} moiety were obtained as optimized structures by molecular orbital calculations. The observed low fluorescence intensity and the short fluorescence lifetime of the C_{60} moiety of these molecular systems indicated that charge separation takes place via the excited singlet state of the C_{60} moiety in a quite fast rate and high efficiency even in the nonpolar solvent toluene, which was a quite new observation compared with reported dyads with different spacers. From the absorption bands at 880 and 1000 nm in the nanosecond transient absorption spectra, generations of $C_{60}^{\bullet-}$-sp-BBA$^{\bullet+}$ and $C_{60}^{\bullet-}$-(sp-BBA$^{\bullet+}$)(sp-BBA) were confirmed. The rates of charge separation and charge recombination for C_{60}-(sp-BBA)$_2$ are faster than those for C_{60}-sp-BBA, suggesting that one of the BBA moieties approaches the C_{60} moiety by pushing another BBA moiety because of the flexible spacers.

Introduction

In one of the most attractive strategies to reach efficient intramolecular electron transfer and to produce long-lived charge-separated states, various electron donors have been covalently connected to the C_{60} cage by different synthetic procedures.[1−8] These C_{60}/donor dyads and triads have been employed as artificial photosynthetic systems,[2,3,5,6,9−11] because of properties of C_{60} π-electron systems, including the small reorganization energy due to spherical molecular shape.[9] Considerable efforts have been devoted in recent years to clarify the photophysical and electrochemical properties of C_{60}/donor dyads and triads[12−17] in addition to the mixture systems of C_{60} and donor.[18−22]

Among a wide variety of donor molecules, bis(biphenyl)-aniline (BBA) is one of the strong electron donors, because BBA forms stable amine radical cation compared with other aromatic amines such as dimethylanilines and triphenylamines. Furthermore, BBA can be used as building blocks for high-spin polyradical and conducting polymers as well as the hole-transfer layer in electroluminescent devices.[23,24] It was reported that BBA acts as a good electron donor with respect to C_{60} in the dyad,[25] generating a quite persistent charge-separated state even in quite short distances between the radical anion and the radical cation. In the case of a dyad with a long rigid spacer, further prolongation of the lifetime of the charge-separated state was observed.[26] In the present study, we prepared C_{60}-sp-BBA and C_{60}-(sp-BBA)$_2$ with a longer flexible linkage as shown in Figure 1. It is interesting that optimized structures of C_{60}-sp-BBA and C_{60}-(sp-BBA)$_2$ with the flexible alkylthioacetamide chain give folded structures, approaching the BBA moiety to the C_{60} moiety. In addition, a two-donor strategy may give additional effects on photoinduced electron transfer.[13,27−29] The charge-separation and recombination processes were investigated by the time-resolved fluorescence and absorption spectra in the visible and near-IR regions. Differences between C_{60}-sp-BBA and C_{60}-(sp-BBA)$_2$ can be discussed in relation to the geometrical factors.

Results and Discussion

Synthesis of C_{60}-(sp-BBA)$_2$ and C_{60}-sp-BBA. C_{60}-(sp-BBA)$_2$ was synthesized as shown in Scheme 1. According to the reported method, dicarboxylic acid (**1**)[26] was treated with oxalyl chloride to yield dicarboxylic acid chloride **2**. The reaction of **2** with triarylamine **3**, which was synthesized by the literature method,[30] afforded the corresponding *N,N*-bis(biphenyl)aniline derivative possessing a masked diene unit as the sulfolene moiety (**4**) in 61% yield in two steps. The Diels−Alder reaction[31] of **4** and C_{60} in refluxing *o*-dichlorobenzene in the presence of hydroquinone gave C_{60}-(sp-BBA)$_2$ in 45% yield. The structure of C_{60}-(sp-BBA)$_2$ was characterized by ^{1}H and ^{13}C NMR, IR, and FAB-MS spectra. Details of the experimental procedures are described in the Supporting Information.

In a similar manner, C_{60}-sp-BBA was obtained by the amide-forming reaction of sulfolene-containing carboxylic acid **5** with

* Authors for correspondence. E-mail: ito@tagen.tohoku.ac.jp. E-mail: ttakata@polymer.titech.ac.jp.
† Tohoku University.
‡ Osaka Prefecture University.
§ Yashima Super Structured Helix Project.
|| Tokyo Institute of Technology.

10.1021/jp052063f CCC: $30.25
Published on Web 08/18/2005

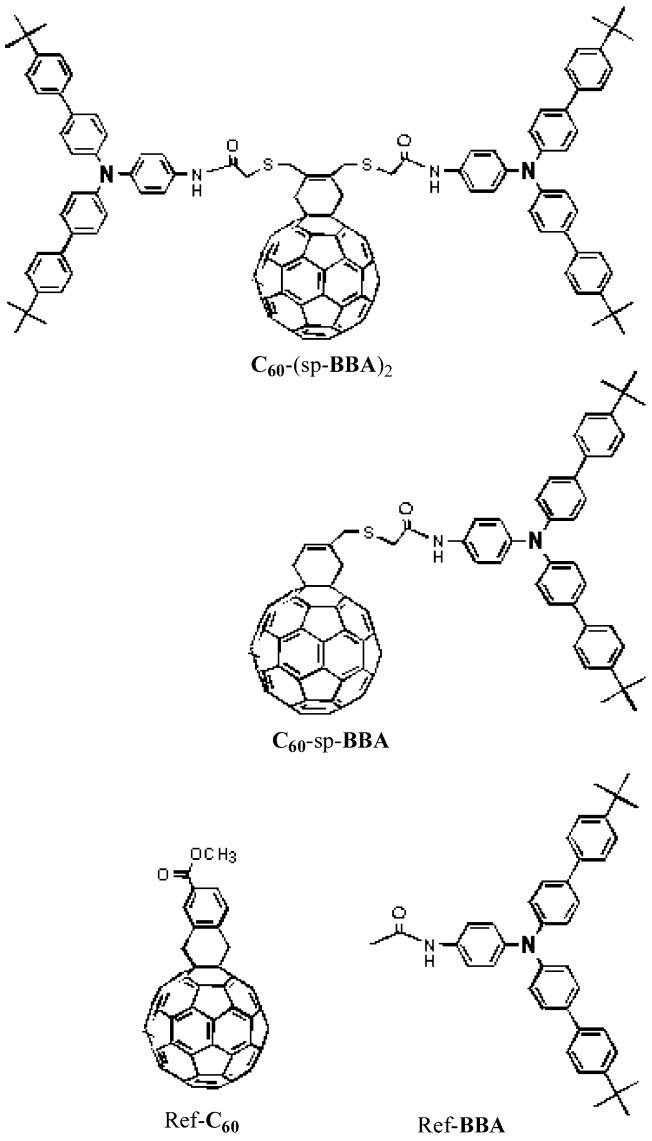

Figure 1. Molecular structures of C_{60}-(sp-BBA)$_2$, C_{60}-sp-BBA, and references.

arylamine **6** with dicyclohexylcarbodiimide (DCC) followed by the Diels−Alder reaction of **7** and [60]fullerene in a good yield (Scheme 2). The structure of C_{60}-sp-BBA was characterized by ^{1}H and ^{13}C NMR, IR, and FAB-MS spectra. Details of the experimental procedures for the syntheses of both **5** and C_{60}-sp-BBA are described in the Supporting Information.

Molecular Orbital Calculations. Figure 2 shows the optimized structures and the electron densities of the lowest unoccupied molecular orbital (LUMO) and the highest occupied molecular orbital (HOMO) of C_{60}-(sp-BBA)$_2$ and C_{60}-sp-BBA calculated by using the density functional B3LYP/6-31G(*) method.

The optimized structures show that the alkylthioacetamide chains used as spacers for C_{60}-sp-BBA and C_{60}-(sp-BBA)$_2$ are quite flexible. Thus, such spacers give folded structures as more stable conformation. The center-to-center distance (R_{CC}) of the BBA and C_{60} moieties with the folded conformations was estimated to be 9.0 Å for C_{60}-sp-BBA, in which the BBA plain is in face-to-face alignment with respect to the C_{60} sphere. In the case of C_{60}-(sp-BBA)$_2$, the R_{CC} value for the near-side BBA moiety is 7.8 Å, which is shorter than that of C_{60}-sp-BBA, suggesting that the near-side BBA was pushed to the C_{60} moiety by another BBA moiety because of steric interference between the two BBA units. The calculated electron densities of the HOMO indicate the delocalization of electrons in the BBA moiety, whereas the electron densities in the LUMO are all located on the C_{60} moiety, suggesting that the BBA and C_{60} moieties act as an electron donor and an electron acceptor, respectively.

Electrochemical Measurements. The cyclic voltammograms of C_{60}-(sp-BBA)$_2$ and C_{60}-sp-BBA in PhCN gave an almost reversible pattern suggesting the stability of the radical ions (see Supporting Information). Compared with the E_{ox} values of ref-BBA ($E_{ox} = +0.35$ V vs Fc/Fc$^+$), the peaks observed for C_{60}-(sp-BBA)$_2$ (+0.33 V vs Fc/Fc$^+$) and C_{60}-sp-BBA (+0.32 V vs Fc/Fc$^+$) were attributed to the E_{ox} values of the BBA moiety; resemblance of the E_{ox} values suggests the absence of an interaction between the BBA and C_{60} moieties in the ground state.

The reduction potential (E_{red}) of C_{60}-(sp-BBA)$_2$ and C_{60}-sp-BBA was evaluated to be −1.03 V vs Fc/Fc$^+$; this value is corresponding to E_{red} of the C_{60} moiety, since a quite similar value was reported for ref-C_{60} ($E_{red} = -1.10$ V vs Fc/Fc$^+$). From these observed E_{ox} and E_{red} values for C_{60}-(sp-BBA)$_2$ and C_{60}-sp-BBA, the free-energy changes for charge recombination (ΔG_{CR}) and charge separation (ΔG_{CS}) can be calculated according to the Weller equations[32]

$$-\Delta G_{CR} = E_{ox} - E_{red} + \Delta G_S \quad (1)$$

$$-\Delta G_{CS} = \Delta E_{0-0} - (-\Delta G_{CR}) \quad (?)$$

$$-\Delta G_S = \frac{e^2}{4\pi\epsilon_0}\left[\left(\frac{1}{2R^+} + \frac{1}{2R^-} - \frac{1}{R_{CC}}\right)\left(\frac{1}{\epsilon_s}\right) - \left(\frac{1}{2R^+} + \frac{1}{2R^-}\right)\left(\frac{1}{\epsilon_r}\right)\right] \quad (3)$$

where ΔE_{0-0} refers to energy of the 0−0 transition of C_{60}, R^+ to radii of the radical cation of BBA, and R^- to radii of the radical anion of C_{60} (Table 1); e, ϵ_0, ϵ_s, and ϵ_r refer to elementary charge, vacuum permittivity, and static permittivities of the solvents used for rate measurements and redox potential measurements, respectively. The ΔG_{CS} and ΔG_{CR} values for C_{60}-(sp-BBA)$_2$ and C_{60}-sp-BBA in PhCN are summarized in Table 1. In polar and nonpolar solvents, the charge-separation process via the excited singlet state of the C_{60} moiety ($^1C_{60}$*) is exothermic and occurs easily. The charge-separation process via the excited triplet state of the C_{60} moiety ($^3C_{60}$*) is slightly exothermic in THF, PhCN, and DMF.

Steady-State Absorption Measurements. UV−vis absorption spectra of C_{60}-(sp-BBA)$_2$ and C_{60}-sp-BBA and its constituent components (ref-BBA and ref-C_{60}) in PhCN are shown in Figure 3. The broad absorption bands at 640 and 710 nm of C_{60}-sp-BBA are characteristic of the 58 conjugated π-electrons of the C_{60} moiety. The BBA moiety shows the absorption in shorter wavelength than 400 nm. Each absorption spectrum of C_{60}-(sp-BBA)$_2$ or C_{60}-sp-BBA is a superposition of those of the reference compounds, indicating no appreciable interaction in the ground state. From the MO calculations, the charge-transfer band would be anticipated in the longer wavelength region than 700 nm; however, the absorption intensity is too low to observe explicitly.

Steady-State Fluorescence Measurement. Steady-state fluorescence spectra of C_{60}-(sp-BBA)$_2$ and C_{60}-sp-BBA in DMF, PhCN, THF, and toluene exhibit the fluorescence peak (λ_f) at 720 nm as shown in Figure 4. Since the spectral shapes of the fluorescence bands of C_{60}-(sp-BBA)$_2$ and C_{60}-sp-BBA are

SCHEME 1: Synthesis of C_{60}-(sp-BBA)$_2$

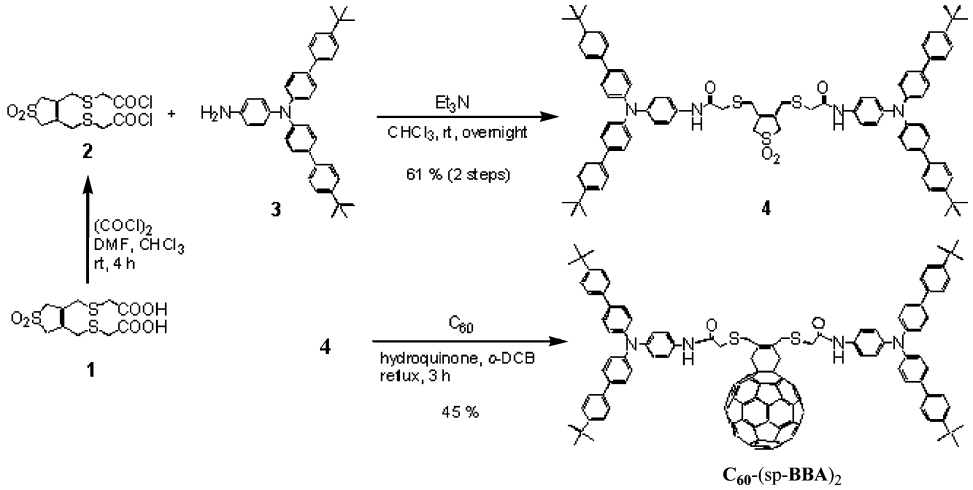

SCHEME 2: Synthesis of C_{60}-sp-BBA

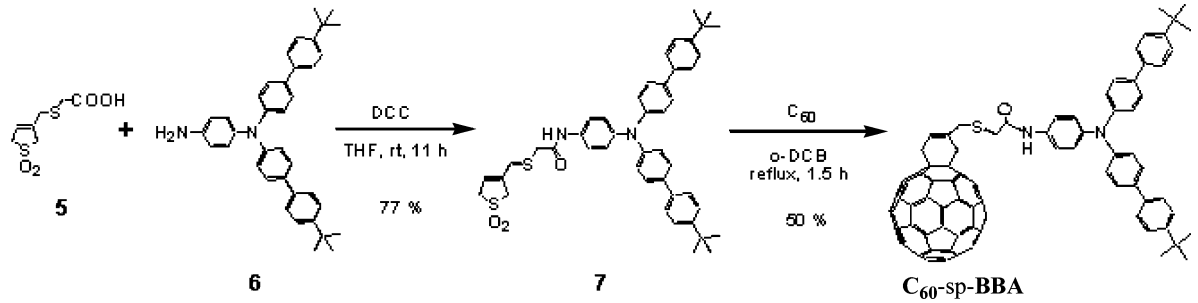

almost the same as that of ref-C_{60} in the same solvents (λ_f = 717 nm), the origin of the observed fluorescence of C_{60}-(sp-BBA)$_2$ and C_{60}-sp-BBA are attributed to the C_{60} moiety. From the cross-point of the fluorescence band and the absorption band after normalizing both intensities, the lowest singlet excited energy (ΔE_{0-0}) of the C_{60} moiety was estimated to be 1.75 eV. Both C_{60}-(sp-BBA)$_2$ and C_{60}-sp-BBA show a weak emission from the C_{60} moiety in DMF, PhCN, THF, and toluene comparing with that from ref-C_{60} in toluene, indicating the efficient quenching of the excited singlet state of the C_{60} moiety, i.e., the peak intensity decreased markedly by a factor of $^1/_{15}$ in toluene, compared with that of ref-C_{60} in toluene. In the case of toluene, there is no spectral evidence for exciplex formation or energy transfer. These observations suggest that the CS process predominantly takes place from $^1C_{60}$* generating $C_{60}^{\bullet-}$-sp-BBA$^{\bullet+}$ and $C_{60}^{\bullet-}$-(sp-BBA$^{\bullet+}$)(sp-BBA) by the excitation with 500-nm light even in the nonpolar solvent toluene. Further quantitative analyses on the fluorescence properties were carried out on the basis of the fluorescence lifetime measurements.

Fluorescence Lifetimes. In Figure 5, the time profiles of the fluorescence intensity at the peak position of the $^1C_{60}$* moiety in C_{60}-(sp-BBA)$_2$ and C_{60}-sp-BBA in toluene and PhCN and ref-C_{60} in toluene are shown. The fluorescence decay of the ref-$^1C_{60}$* moiety obeys a single-exponential function, yielding the fluorescence lifetime (τ_f) of 1400 ps in toluene.[33] The time profiles of the fluorescence at 720 nm of the C_{60} moiety in C_{60}-(sp-BBA)$_2$ and C_{60}-sp-BBA show biexponential decay in DMF, PhCN, THF, and toluene; a major component decayed with the τ_f values in the 80 ps (75%) to 90 ps (60%) region, whereas minor slow decay components gave τ_f values of 1300 ps. The τ_f values of the major components are summarized in Table 2.

The difference between the τ_f values evaluated from the main fluorescence decays in 710−730 nm in polar and nonpolar solvents can be attributed predominantly to charge separation via the $^1C_{60}$* moiety in C_{60}-(sp-BBA)$_2$ and C_{60}-sp-BBA, generating the radical ion-pair states ($C_{60}^{\bullet-}$-sp-BBA$^{\bullet+}$ and $C_{60}^{\bullet-}$-(sp-BBA$^{\bullet+}$)(sp-BBA)). From the τ_f value of the $^1C_{60}$* moiety in both compounds, the intramolecular charge-separation rate constants (k_{CS}^S) in polar and nonpolar solvents were evaluated as summarized in Table 2 using the following relation

$$k_{CS}^S = (1/\tau_f)_{sample} - (1/\tau_0)_{ref} \quad (4)$$

where $(\tau_0)_{ref}$ is the fluorescence lifetime of ref-C_{60} in toluene.[31] Thus, the k_{CS}^S values for C_{60}-(sp-BBA)$_2$ and C_{60}-sp-BBA were evaluated to be (1.2−2.1) × 10^{10} s^{-1} and (1.0−1.3) × 10^{10} s^{-1}, respectively, which indicate that charge separation via the $^1C_{60}$* moiety is an effective process in polar and nonpolar solvents. The quantum yields of the charge separation (Φ_{CS}^S) via the $^1C_{60}$* moiety in C_{60}-(sp-BBA)$_2$ and C_{60}-sp-BBA were evaluated from eq 5

$$\Phi_{CS}^S = [(1/\tau_f)_{sample} - (1/\tau_0)_{ref}]/(1/\tau)_{sample} \quad (5)$$

Thus, Φ_{CS}^S = 0.71−0.97 and 0.56−0.95 were calculated for C_{60}-(sp-BBA)$_2$ and C_{60}-sp-BBA (Table 2) in polar and nonpolar solvents, respectively, which indicates that the charge separation via the $^1C_{60}$* moiety is the main process, overwhelming the intersystem crossing (ISC) process to the $^3C_{60}$* moiety even in toluene. Table 3 indicates that the k_{CS}^S and Φ_{CS}^S values in both compounds slightly decreased with solvent polarity.

Nanosecond Transient Absorption Measurements. Transient absorption spectra observed by the nanosecond laser excitation with the 532-nm light, which predominantly excites the C_{60} moiety of C_{60}-(sp-BBA)$_2$ and C_{60}-sp-BBA in PhCN, are shown in Figure 6. The broad absorption bands were observed in the region of 650−1100 nm, which is the overlap-

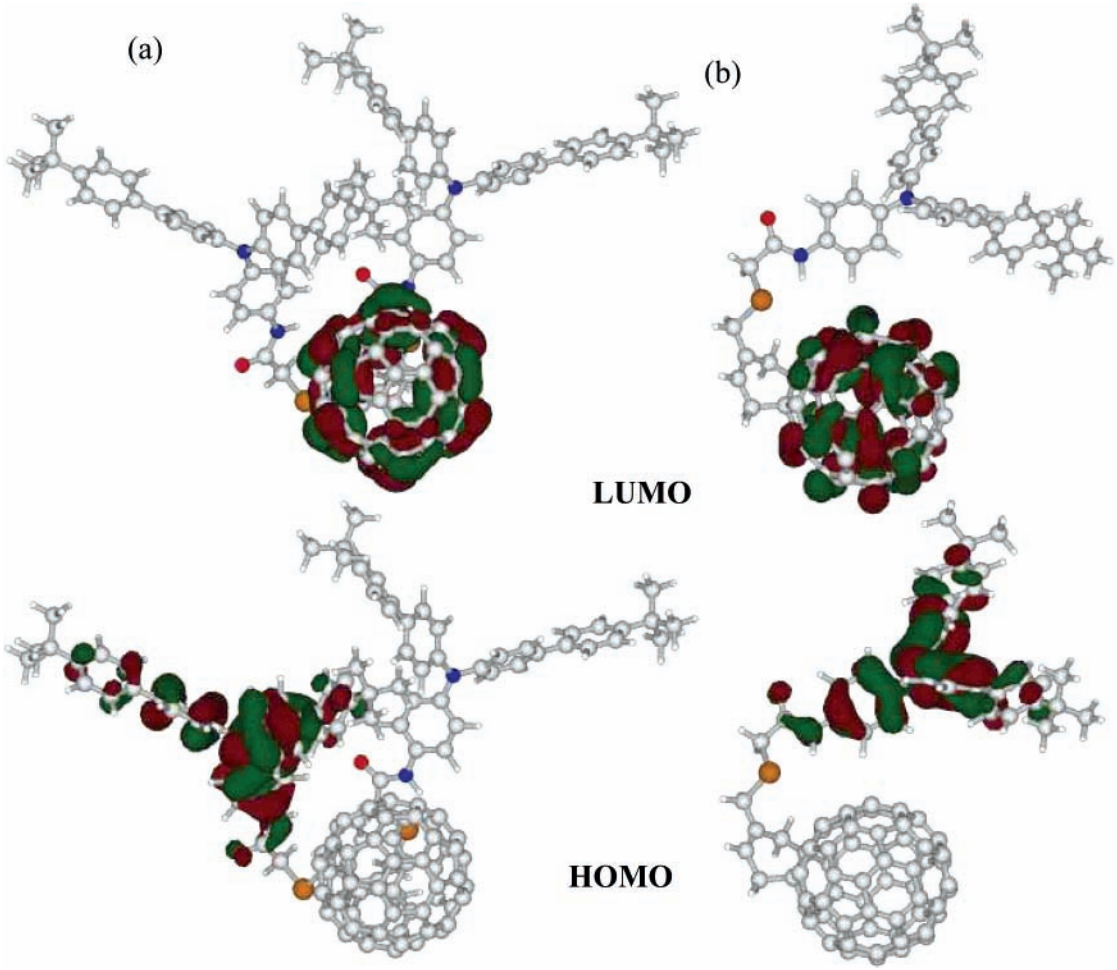

Figure 2. Optimized structures and electron distributions of LUMO and HOMO of (a) C_{60}-(sp-BBA)$_2$ and (b) C_{60}-sp-BBA calculated at B3LYP/6-31G(*)+1 level.

TABLE 1: Free-Energy Change for Charge Separation ($-\Delta G_{CS}$) and Free-Energy Change for Charge Recombination ($-\Delta G_{CR}$) of C_{60}-(sp-BBA)$_2$ and C_{60}-sp-BBA

sample	solvent	$-\Delta G^{S}_{CS}$/eV	$-\Delta G_{CR}{}^{a}$/eV
C_{60}-(sp-BBA)$_2$	DMF	0.47	1.28
	PhCN	0.46	1.29
	THF	0.40	1.35
	TN	0.21	1.54
C_{60}-sp-BBA	DMF	0.48	1.27
	PhCN	0.46	1.29
	THF	0.38	1.37
	TN	0.12	1.63

[a] Calculated from eqs 1−3 employing $\Delta E_{0-0} = 1.75$ eV for $^1C_{60}$*, $\Delta E_{0-0} = 1.52$ eV for $^3C_{60}$*, $E_{ox} = 0.33$, 0.32 V for BBA, and $E_{red} = -1.03$, −1.03 V for C_{60} vs Fc/Fc$^+$ of C_{60}-(sp-BBA)$_2$ and C_{60}-sp-BBA in PhCN, respectively. $R^+ = 7.4$ Å for BBA, and $R^- = 4.7$ Å for C_{60}, and $R_{CC} = 7.8$ Å for C_{60}-(sp-BBA)$_2$ and 9.0 Å for C_{60}-sp-BBA as evaluated from Figure 2. Permittivities of toluene, THF, PhCN, and DMF are 2.38, 7.58, 25.2, and 37, respectively.

ping region of the absorption bands of the BBA$^{\bullet+}$ moiety (880 nm)[25] and the $C_{60}^{\bullet-}$ moiety (1000 nm).[18] From the decay time profiles at 1020 nm, the charge-recombination rate constants (k_{CR}) were evaluated to be 4.0×10^6 s^{-1} for C_{60}-(sp-BBA)$_2$ and 3.0×10^6 s^{-1} for C_{60}-sp-BBA, from which the lifetimes (τ_{RIP}) of the charge-separated states were calculated to be 250 and 330 ns in PhCN, respectively, at room temperature as listed in Table 3. Thus, the k_{CR} value for C_{60}-(sp-BBA)$_2$ is greater than that for C_{60}-sp-BBA.

In other polar solvents such as DMF and THF, similar transient spectra to those in PhCN were observed, showing the generation of the charge-separated states. The solvent polarity effect on the τ_{RIP} values was significant as listed in Table 3; for both C_{60}-(sp-BBA)$_2$ and C_{60}-sp-BBA, the tendency of the τ_{RIP} values in DMF < in PhCN < in THF is found.

In toluene, transient absorption spectra were observed as shown in Figure 7. At 7 ns after the laser exposure, the transient absorption band appeared at 1000 nm, although the decay was quite quick. This observation was supported by the negative ΔG^{S}_{CS} value in toluene (Table 1), suggesting the formation of the radical ion pair ($C_{60}^{\bullet-}$-(sp-BBA$^{\bullet+}$)(sp-BBA) and $C_{60}^{\bullet-}$-sp-BBA$^{\bullet+}$) in toluene. At 100 ns, the broad band appearing at 700 nm with slow decay can be attributed to the $^3C_{60}$* moiety.[22] Since the absorption intensities of the $^3C_{60}$* moiety of C_{60}-(sp-BBA)$_2$ and C_{60}-sp-BBA were considerably lower than that of ref-C_{60} in toluene under the same experimental conditions (see Supporting Information), some of the parts of the $^1C_{60}$* moiety go to the charge separation competitively with ISC to the $^3C_{60}$* moiety. The average Φ^{S}_{CS} values (0.71 for C_{60}-(sp-BBA)$_2$ and 0.56 for C_{60}-sp-BBA) in toluene are in agreement with the low ratio of the generation of $^3C_{60}$* via ISC. Furthermore, the inserted time profiles (Figure 7) at 1000 nm showing quick decay of $C_{60}^{\bullet-}$-(sp-BBA$^{\bullet+}$)(sp-BBA) and $C_{60}^{\bullet-}$-sp-BBA$^{\bullet+}$ in the time region until ca. 20 ns obey first-order kinetics with rate constants of 1.2×10^8 s^{-1} and 1.1×10^8 s^{-1}, respectively, at room temperature. These τ_{RIP} values (<10 ns) are significantly shorter than the τ_{RIP} values in polar solvents such as DMF, PhCN, and THF, which are capable of fully solvating the radical

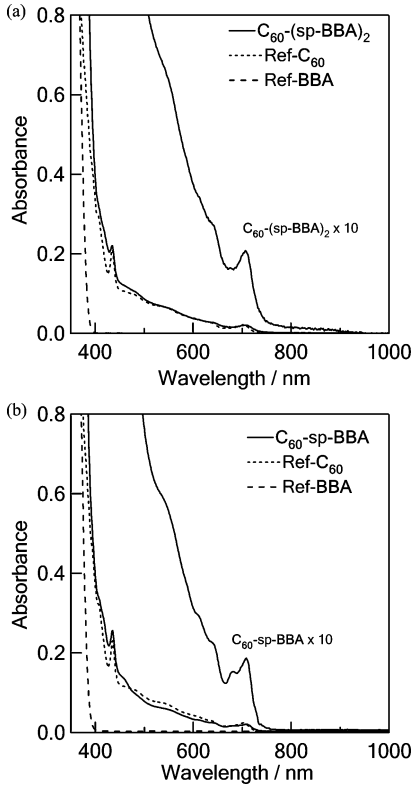

Figure 3. Steady-state absorption spectra of (a) C_{60}-(sp-BBA)$_2$ and (b) C_{60}-sp-BBA in addition to reference compounds in PhCN; concentration = 0.1 mM.

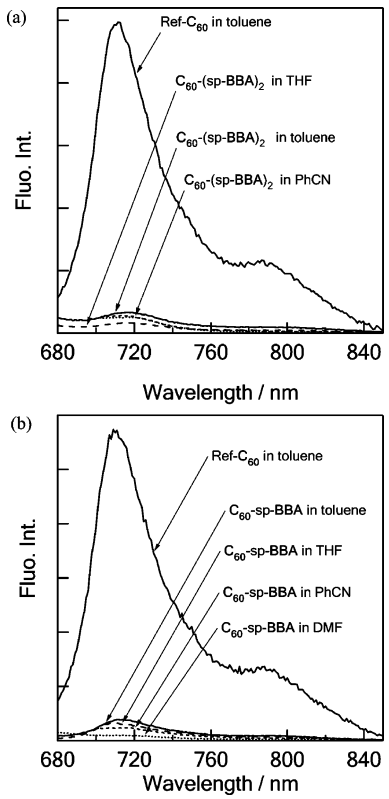

Figure 4. Steady-state fluorescence spectra of (a) C_{60}-(sp-BBA)$_2$ (0.1 mM) and (b) C_{60}-sp-BBA and reference samples (0.1 mM) in toluene, THF, PhCN, and DMF and ref-C_{60} (0.1 mM) in toluene; λ_{ex} = 500 nm.

ion pair.[25,26] In toluene, on the other hand, the charge-separated states are not fully solvated, giving short lifetimes.

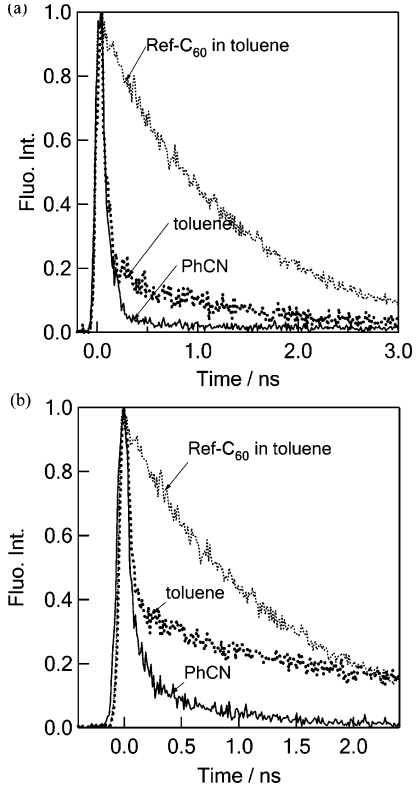

Figure 5. Fluorescence decay profiles around 710−730 nm of (a) C_{60}-(sp-BBA)$_2$ (0.1 mM) and (b) C_{60}-sp-BBA (0.1 mM) in toluene and PhCN and ref-C_{60} (0.1 mM) in toluene after 410-nm laser irradiation.

TABLE 2: Fluorescence Lifetime (τ_f at 700−800 nm), Charge Separation Rate Constant (k_{CS}^S), Quantum Yield for Charge Separation (Φ_{CS}^S), via $^1C_{60}$* of C_{60}-(sp-BBA)$_2$ and C_{60}-sp-BBA

sample	solvent	τ_f/ps	k_{CS}^S[a]/s^{-1}	Φ_{CS}^S[a]
C_{60}-(sp-BBA)$_2$	DMF	50	2.1×10^{10}	0.97
	PhCN	55	1.8×10^{10}	0.96
	THF	70	1.4×10^{10}	0.95
	TN	80 (75%)	1.2×10^{10}	0.94 (0.70)[b]
C_{60}-sp-BBA	DMF	70	1.3×10^{10}	0.95
	PhCN	75	1.3×10^{10}	0.95
	THF	80	1.2×10^{10}	0.94
	TN	90 (60%)	1.0×10^{10}	0.94 (0.56)[b]

[a] Lifetime (τ_{f0}) of reference was evaluated to be 1390 ps (ref-C_{60} in toluene), The k_{CS}^S and Φ_{CS}^S were calculated from eqs 3 and 4. [b] Average values including the slow fluorescence lifetimes.

TABLE 3: Charge Recombination Rate Constant (k_{CR}) and Lifetime (τ_{RIP}) of C_{60}-(sp-BBA)$_2$ and C_{60}-sp-BBA

sample	solvent	k_{CR}/s^{-1}	τ_{RIP}/ns
C_{60}-(sp-BBA)$_2$	DMF	6.20×10^6	160
	PhCN	4.00×10^6	250
	THF	3.10×10^6	320
	TN	1.20×10^8	<10
C_{60}-sp-BBA	DMF	5.50×10^6	180
	PhCN	3.00×10^6	330
	THF	2.60×10^6	390
	TN	1.10×10^8	<10

Energy Diagram. Figure 8 shows an energy diagram of C_{60}-(sp-BBA)$_2$ when the 532-nm laser light is used as the excitation light. Energy levels of the radical ion pairs are cited from the ΔG_{CR} values in Table 1. A similar energy diagram can be depicted for C_{60}-sp-BBA. In polar and nonpolar solvents, the charge separation takes place via $^1C_{60}$*-(sp-BBA)$_2$ and $^1C_{60}$*-sp-BBA, since the energy levels of $C_{60}^{\bullet-}$-(sp-BBA$^{\bullet+}$)(sp-BBA)

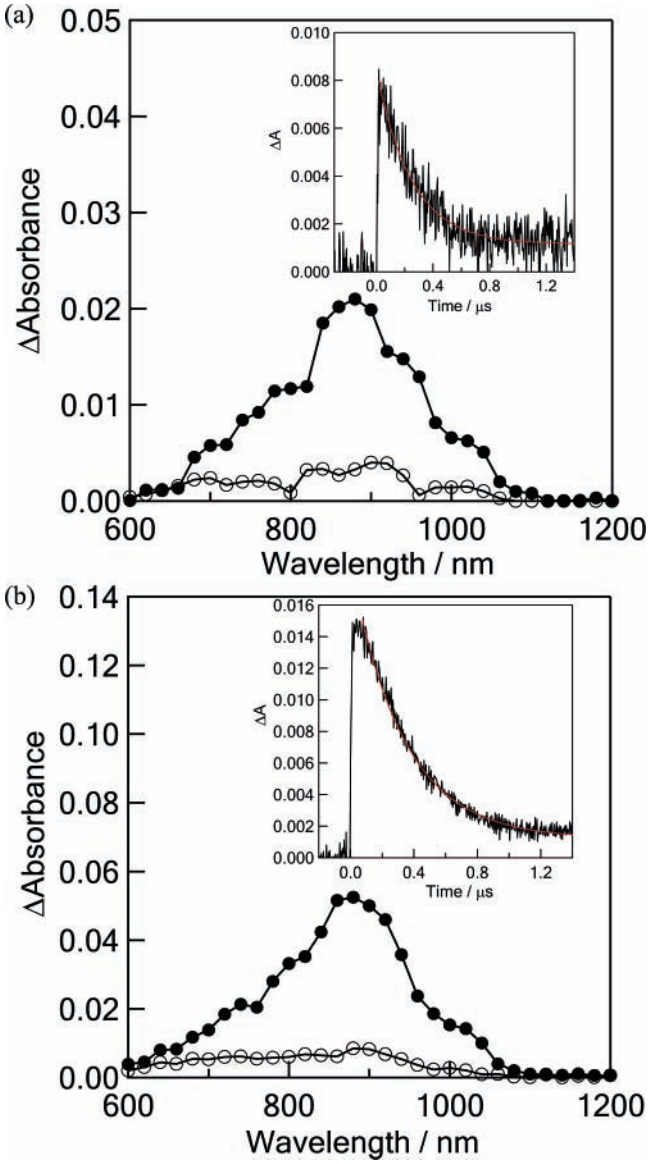

Figure 6. Nanosecond transient absorption spectra of (a) C_{60}-(sp-BBA)$_2$ (0.1 mM) and (b) C_{60}-sp-BBA (0.1mM) observed by 532-nm laser irradiation in at 0.1 μs (●) and 1.0 μs (○) in PhCN. Inset: Absorption−time profiles at 1020 nm in PhCN.

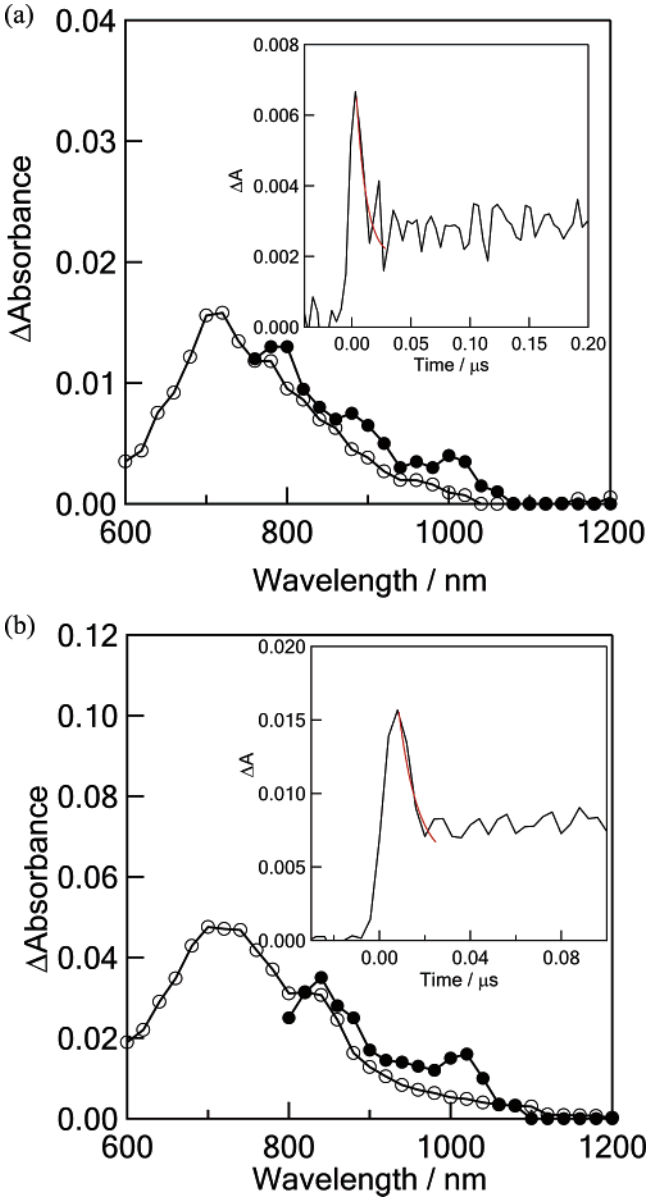

Figure 7. Nanosecond transient absorption spectra of (a) C_{60}-(sp-BBA)$_2$ (0.1 mM) and (b) C_{60}-sp-BBA (0.1mM) observed by 532-nm laser irradiation in at 5 ns (●) and 100 ns (○) in toluene at room temperature. Inset: Absorption−time profiles at 1000 nm in toluene.

and $C_{60}^{\bullet-}$-sp-BBA$^{\bullet+}$ were lower than those for $^1C_{60}$*-(sp-BBA)$_2$ and $^1C_{60}$*-sp-BBA. In the case of the nonpolar solvent toluene, the charge-separation process via $^1C_{60}$* occurs competitively with the ISC process; Φ_{ISC} can be calculated as $(1 - \Phi_{CS}^S)$ from Table 2. Thus, the Φ_{ISC} values of $^1C_{60}$*-(sp-BBA)$_2$ and $^1C_{60}$*-sp-BBA were calculated as 0.29 and 0.40, respectively. Since the energy levels of $C_{60}^{\bullet-}$-(sp-BBA$^{\bullet+}$)(sp-BBA) and $C_{60}^{\bullet-}$-sp-BBA$^{\bullet+}$ in polar solvents are lower than that of the $^3C_{60}$* moiety, charge separation via the $^3C_{60}$* moiety is thermodynamically possible. However, the Φ_{CS}^S values are higher than 0.94 in polar solvent and the population of the $^3C_{60}$* moiety is quite less; thus, charge separation via the $^3C_{60}$* moiety is practically unobservable. In toluene, charge separation via the $^3C_{60}$* moiety is thermodynamically impossible. The k_{CR} values tend to decrease with solvent polarity as seen in Table 3, suggesting that the charge-recombination process is in the inverted region of the Marcus parabola.[34] This is reasonable from the ΔG_{CR} values that are more negative than −1.2 eV, since the reorganization energies for the charge recombination of the C_{60} derivatives are reported to be 0.5−0.7 eV.[9,15b,25]

Comparison of C_{60}-(sp-BBA)$_2$ with C_{60}-sp-BBA. In each solvent, the k_{CS}^S and Φ_{CS}^S values for C_{60}-(sp-BBA)$_2$ are larger than the corresponding values for C_{60}-sp-BBA, indicating that a short distance between donor and acceptor for C_{60}-(sp-BBA)$_2$ results in higher efficiency in the charge separation. Furthermore, the k_{CR} value for C_{60}-(sp-BBA)$_2$ is larger than the corresponding value for C_{60}-sp-BBA, indicating that the close configuration of the BBA and C_{60} moieties in C_{60}-(sp-BBA)$_2$ accelerates the charge recombination, too.

Comparison with Other C_{60}-sp-BBA Systems. The geometrical data and kinetic data for other C_{60}-sp-BBA systems are summarized in Table 4. The k_{CS}^S values increase with a decrease in the nearest distances (R_{near}) between the electron clouds of the HOMO of the BBA moiety and the LUMO of the C_{60} moiety, which can be explained by the increase in the electron-coupling matrix element of the Marcus theory, because the charge separation took place on the top region of Marcus parabola;[34] that is, the k_{CS} values are proportional to the square of the coupling matrix element on the top region. On the other

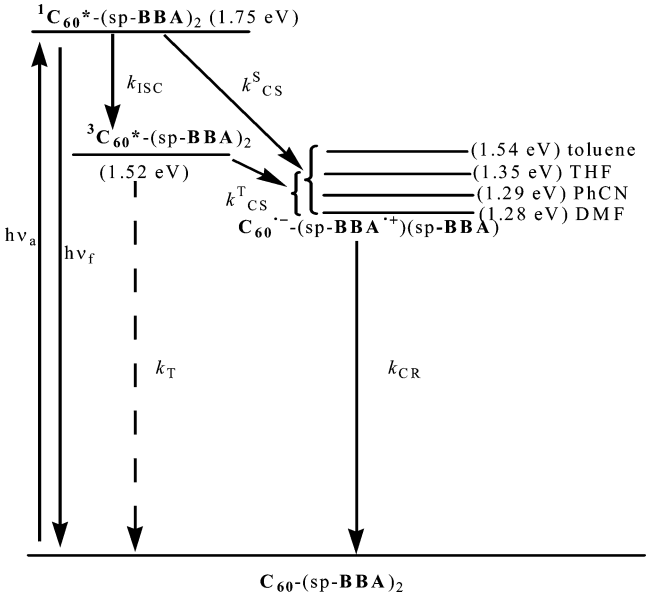

Figure 8. Schematic energy diagram for electron-transfer processes of C_{60}-(sp-BBA)$_2$ in toluene, THF, PhCN, and DMF.

TABLE 4: Distances (R_{CC} and R_{near}), k^S_{CS}, k_{CR}, and k^S_{CS}/k_{CR} of Various C_{60}-sp-BBA in PhCN

sample	R_{CC}/Å	R_{near}/Å	k^S_{CS}/s^{-1}	k_{CR}/s^{-1}	k^S_{CS}/k_{CR}
C_{60}-sp-BBA[a]	7.9	3.4	1.3×10^{10}	3.0×10^6	4300
C_{60}-(sp-BBA)$_2$[a]	9.0	2.3	1.8×10^{10}	4.0×10^6	4500
C_{60}-sp$_1$-BBA[b]	12.4	1.9	5.0×10^{10}	4.5×10^6	11000
C_{60}-sp$_2$-BBA[c]	15.0	7.1	3.0×10^9	3.1×10^6	1000
C_{60}-TPA[d]	11.0	1.5	7.3×10^9	$<1.67 \times 10^8$	43

[a] Present study. [b] ref 25 [c] ref 26. [d] TPA (triphenylamine) ref 35.

hand, the k_{CR} values are almost the same even when changing the R_{CC} and R_{near} values. Since the charge-recombination process is in the inverted region, the distant dependence for k_{CR} may be more complex, because the solvent reorganization energy also depends on the R_{CC} or R_{near} values. Therefore, the observed ratio of k^S_{CS}/k_{CR}, which is a measure of the light conversion efficiency to charge-separated states, shows a maximum at appropriate R_{CC} and R_{near} values. On the basis of this viewpoint, C_{60}-(sp-BBA)$_2$ and C_{60}-sp-BBA with the flexible spacer studied in the present study are better than C_{60}-sp$_2$-BBA with a rigid spacer in our previous report.[26]

Comparison with Other C_{60} Systems. In comparison with aromatic donors such as dimethyl aniline and diphenyl aniline, the BBA moiety has excellent donor ability, giving persistent radical ion pairs, irrespective of the distance between the amine and C_{60} moieties. For example, for the NMPC_{60}−TPA dyad, the τ_{RIP} value was less than 10 ns.[35] In the case of a triad composed of NMPC_{60}−quaterthiophene−TPA, the τ_{RIP} value was evaluated to be 18 ns in DMF at room temperature.[36] The τ_{RIP} value for a triad composed of the C_{60}−fluorene−diphenylamine was evaluated to be 150 ns in DMF at room temperature.[37] In the case of C_{60}−bridge−dimethylaniline systems, τ_{RIP} values in the range 8−250 ns were reported, depending on the kinds and lengths of the bridge molecules.[7] In comparison to these C_{60} and amine systems, $C_{60}^{\bullet-}$-sp-BBA$^{\bullet+}$ showed a long τ_{RIP} value.

Summary

For C_{60}-sp-BBA and C_{60}-(sp-BBA)$_2$, in which the flexible covalent bonds are employed as a spacer, photoinduced charge separation via $^1C_{60}$* was observed in polar solvents at room temperature. The efficiency and rate of the charge-separation process are quite high. The longest lifetimes for $C_{60}^{\bullet-}$-(sp-BBA$^{\bullet+}$)(sp-BBA) and $C_{60}^{\bullet-}$-sp-BBA$^{\bullet+}$ were 320 and 390 ns, respectively, in THF at room temperature. It is revealed that a smaller λ value than the absolute values of ΔG_{CR} leads to the inverted region of the Marcus parabola, resulting in slowing down the charge recombination rate.

Experimental Section

Materials. [60]Fullerene (C_{60}) was obtained from MER Corporation, U.S.A. (99.5% purity). PhCN, toluene, *n*-hexane, benzene-d_6, *N*-methyl glycine, and α-cyano-4-hydroxycinnamic acid were purchased from Aldrich Chemicals (Milwaukee, WI).

Synthesis. Ref-C_{60},[26] ref-BBA,[26] and compounds **1**,[26] **2**,[26] and **3**[30] were prepared by the methods reported elsewhere. Both C_{60}-(sp-BBA)$_2$ and C_{60}-sp-BBA were synthesized according to Schemes 1 and 2. The experimental procedures are described in the Supporting Information. The characteristics of the two compounds are shown below.

C_{60}-(sp-BBA)$_2$. ^{1}H NMR (400 MHz, $CDCl_3$) δ 8.74 (s, 1H), 7.52−7.43 (m, 28H), 7.22−7.16 (m, 12H), 4.09 (s, 4H), 3.98 (s, 4H), 3.87 (s, 4H), 1.36 (s, 36H) ppm; ^{13}C NMR (100 MHz, $CDCl_3$) δ 168.7, 156.6, 149.9, 147.9, 146.61, 146.56, 146.3, 145.9, 145.5, 144.8, 143.2, 142.7, 142.4, 142.3, 142.1, 141.7, 140.24, 140.19, 137.7, 135.7, 135.3, 130.9, 129.7, 128.8, 127.7, 127.1, 126.3, 125.7, 123.9, 121.0, 66.0, 38.8, 36.5, 35.1, 34.5, 31.4 ppm; FAB-MS (matrix: mNBA) *m*/*z* 1995 $[M]^+$.

C_{60}-sp-BBA. ^{1}H NMR (400 MHz, $CDCl_3$) δ 8.63 (s, 1H), 7.58−7.43 (m, 14H), 7.22−7.15 (m, 6H), 6.82 (t, J = 5.6 Hz, 1H), 4.11 (s, 2H), 4.03 (d, J = 5.6 Hz, 2H), 3.80 (s, 2H), 3.58 (s, 2H), 1.36 (s, 18H) ppm; ^{13}C NMR (100 MHz, $CDCl_3$) δ 166.5, 157.0, 156.9, 149.9, 147.74, 147.70, 146.6, 146.5, 146.3, 145.8, 145.5, 145.4, 145.3, 144.8, 144.7, 143.2, 142.6, 142.4, 142.2, 142.11, 142.08, 141.7, 140.22, 140.18, 138.6, 137.7, 135.6, 135.5, 135.3, 129.3, 127.7, 126.3, 125.7, 125.4, 123.9, 121.0, 65.84, 65.76, 43.1, 40.5, 39.1, 36.2, 34.5, 31.4 ppm; IR (KBr) 2954, 2923, 1508, 1495, 819 cm^{-1}; FAB-MS (matrix: mNBA) *m*/*z* 1384 $[M]^+$.

Measurements. Electrochemical Measurements. Reduction potentials (E_{red}) and oxidation potentials (E_{ox}) were measured by cyclic voltammetry with a potentiostat (BAS CV50W) in a conventional three-electrode cell equipped with Pt working and counter electrodes with an Ag/Ag^+ reference electrode at scan rate of 100 mV/s. The E_{red} and E_{ox} were expressed vs ferrocene/ferrocenium (Fc/Fc^+) used as the internal reference. In each case, a solution containing 0.2 mM of sample with 0.05 M of *n*-Bu_4NClO_4 (Fluka purest quality) was deaerated with argon bubbling before measurements.

Steady-State Measurements. Steady-state absorption spectra in the visible and near-IR regions were measured on a Jasco V570 DS spectrophotometer. Steady-state fluorescence spectra were measured on a Shimadzu RF-5300 PC spectrofluorophotometer equipped with a photomultiplier tube having high sensitivity in the 700−800 nm region.

Time-Resolved Fluorescence Measurements. The time-resolved fluorescence spectra were measured by the single-photon counting method using a streakscope (Hamamatsu Photonics, C4334-01) as a detector and the laser light (second harmonic generation (SHG), 410 nm) of a Ti:sapphire laser (Spectra-Physics, Tsunami 3950-L2S, 1.5 ps fwhm) as an excitation source.[38] Lifetimes were evaluated with software attached to the equipments.

Nanosecond Transient Absorption Measurements. Nanosecond transient absorption measurements were carried out using

SHG (532 nm) of a Nd:YAG laser (Spectra-Physics, Quanta-Ray GCR-130, 5 ns fwhm) as an excitation source. For transient absorption spectra in the near-IR region (600−1200 nm) and the time profiles, monitoring light from a pulsed Xe lamp was detected with a Ge-APD (Hamamatsu Photonics, B2834). For spectra in the visible region (400−1000 nm), a Si-PIN photodiode (Hamamatsu Photonics, S1722−02) was used as a detector. [22,38]

Molecular Orbital Calculations. The optimized structure, energy levels of the molecular orbitals, and electron densities were calculated by *GAUSSIAN 98* (B3LYP/6-31G(*) level).

Acknowledgment. The present work was supported by a Grant-in-Aid on Scientific Research on Priority Areas (417) from the Ministry of Education, Culture, Sports, Science and Technology of Japan.

Supporting Information Available: Detailed synthetic procedures of both C_{60}-(sp-BBA)$_2$ and C_{60}-sp-BBA, space-filled molecular structures, cyclic voltammograms, and nanosecond transient spectra of ref-C_{60}. This material is available free of charge via the Internet at http://pubs.acs.org.

References and Notes

(1) (a) Foote, C. S. In *Topics in Current Chemistry; Photophysical and Photochemical Properties of Fullerenes*; Series 169; Matty, J., Ed.; Springer-Verlag: Berlin, 1994; p 347. (b) *Fullerene, Chemistry, Physics and Technology*; Kadish, K. M., Ruoff, R. S., Eds.; Wiley-Interscience: New York, 2000.

(2) Sariciftci, N. S.; Wudl, F.; Heeger, A. J.; Maggini, M.; Scorrano, G.; Prato, M.; Bourassa, J.; Ford, P. C. *Chem. Phys. Lett.* **1995**, *247*, 510.

(3) (a) Imahori, H.; Sakata, Y. *Adv. Mater.* **1997**, *9*, 537. (b) Martín, N.; Sánchez, L.; Illescas, B.; Pérez, I. *Chem. Rev.* **1998**, *98*, 2527. (c) Prato, M.; Maggini, M. *Acc. Chem. Res.* **1998**, *31*, 519. (d) Diekers, M.; Hirsch, A.; Pyo, S.; Rivera, J.; Echegoyen, L. *Eur. J. Org. Chem.* **1998**, *63*, 1111. (e) Guldi, D. M.; Prato, M. *Acc. Chem. Res.* **2000**, *33*, 695. (f) Gust, D.; Moore, T. A.; Moore, A. L. *Acc. Chem. Res.* **2001**, *34*, 40.

(4) (a) Yamada, K.; Imahori, H.; Nishimura, Y.; Yamazaki, I.; Sakata, Y. *Chem. Lett.* **1999**, 895. (b) Hutchison, K.; Gao, J.; Schick, G.; Rubin, Y.; Wudl, F. *J. Am. Chem. Soc.* **1999**, *121*, 5611. (c) Mattoussi, H.; Rubner, M. F.; Zhou, F.; Kumar, J.; Tripathy, S. K.; Chiang, L. Y. *Appl. Phys. Lett.* **2000**, *77*, 1540.

(5) (a) Guldi, D. M. *Chem. Commun.* **2000**, 321. (b) Imahori, H.; Sakata, Y. *Eur. J. Org. Chem.* **1999**, 64, 2445. (c) Jolliffe, K. A.; Langford, S. J.; Ranasinghe, M. G.; Shephard, M. J.; Paddon-Row, M. N. *J. Org. Chem.* **1999**, *64*, 1238.

(6) (a) Martín, N.; Sánchez, L.; Guldi, D. M. *Chem. Commun.* **2000**, 113. (b) Guldi, D. M.; Luo, C.; Prato, M.; Dietel, E.; Hirsch, A. *Chem. Commun.* **2000**, 373. (c) Guldi, D. M.; Gonzalez, S.; Martín, N.; Antón, A.; Garín, J.; Orduna, J. *J. Org. Chem.* **2000**, *65*, 1978.

(7) (a) Williams, R. M.; Zwier, M. N.; Verhoeven, J. W. *J. Am. Chem. Soc.* **1995**, *117*, 4093. (b) Williams, R. M.; Koeberg, M.; Lawson, J. M.; An, Y.-Z.; Rubin, Y.; Paddon-Row, M. N.; Verhoeven, J. W. *J. Org. Chem.* **1996**, *61*, 5055.

(8) (a) Thomas, K. G.; Biju, V.; George, M. V.; Guldi, D. M.; Kamat, P. V. *J. Phys. Chem. A* **1998**, *102*, 5341. (b) Thomas, K. G.; Biju, V.; Guldi, D. M.; Kamat, P. V.; George, M. V. *J. Phys. Chem. B* **1999**, *103*, 8864. (c) Thomas, K. G.; Biju, V.; Guldi, D. M.; Kamat, P. V.; George, M. V. *J. Phys. Chem. A* **1999**, *103*, 10755.

(9) Imahori, H.; Hagiwara, K.; Akiyama, T.; Akoi, M.; Taniguchi, S.; Okada, T.; Shirakawa, M.; Sakata, Y. *Chem. Phys. Lett.* **1996**, *263*, 545.

(10) (a) Imahori, H.; Ozawa, S.; Uchida, K.; Takahashi, M.; Azuma, T.; Ajavakom, A.; Akiyama, T.; Hasegawa, M.; Taniguchi, S.; Okada, T.; Sakata, Y. *Bull. Chem. Soc. Jpn.* **1999**, *72*, 485. (b) Imahori, H.; Tamaki, K.; Guldi, D. M.; Luo, C.; Fujitsuka, M.; Ito, O.; Sakata, Y.; Fukuzumi, S. *J. Am. Chem. Soc.* **2001**, *123*, 2607.

(11) (a) Lindell, P. A.; Kuciauskas, D.; Sumida, J. P.; Nash, B.; Nguyen, D.; Moore, A. L.; Moore, T. A.; Gust, D. *J. Am. Chem. Soc.* **1997,** *119*, 1400. (b) Carbonera, D.; Valentin, M.; Corvaja, C.; Agostini, G.; Giacometti, G.; Liddell, P. A.; Kuciauskas, D.; Moore, A. L.; Moore, T. A.; Gust, D. *J. Am. Chem. Soc.* **1998**, *120*, 4398.

(12) (a) Samanta, A.; Kamat, P. V. *Chem. Phys. Lett.* **1992**, *199*, 635. (b) Guldi, D. M.; Maggini, M.; Scorrano, G.; Prato, M. *J. Am. Chem. Soc.* **1997**, *119*, 974. (c) Maggini, M.; Guldi, D. M.; Mondini, S.; Scorrano, G.; Paolucci, F.; Ceroni, P.; Roffia, S. *Chem.—Eur. J.* **1998**, *4*, 1992. (d) Polese, A.; Mondini, S.; Bianco, A.; Toniolo, C.; Scorrano, G.; Guldi, D. M.; Maggini, M. *J. Am. Chem. Soc.* **1999**, *121*, 3446.

(13) Llacay, J.; Veciana, J.; Vidal-Gancedo, J.; Bourdelnde, J. L.; Gonzalez-Moreno, R.; Rovia, C. *J. Org. Chem.* **1998**, *63*, 5201.

(14) Tkachenko, N. V.; Rantala, L.; Tauber, A. Y.; Helaja, J.; Hynninen, P. V.; Lemmetyinen, H. *J. Am. Chem. Soc.* **1999**, *121*, 9378.

(15) Schuster, D. I.; Cheng, P.; Wilson, S. R.; Prokhorenko, V.; Katterle, M.; Holzwarth, A. R.; Braslavsky, S. E.; Klihm, G.; Williams, R. M.; Luo, C. *J. Am. Chem. Soc.* **1999**, *121*, 11599.

(16) (a) Yamashiro, T.; Aso, Y.; Otsubo, T.; Tang, H.; Harima, T.; Yamashita, K. *Chem. Lett.* **1999**, 443. (b) Fujitsuka, M.; Ito, O.; Yamashiro, T.; Aso, Y.; Otsubo, T. *J. Phys. Chem. A* **2000**, *104*, 4876. (d) Fujitsuka, M.; Matsumoto, K.; Ito, O.; Yamashiro, T.; Aso, Y.; Otsubo, T. *Res. Chem. Intermed.* **2001**, *27*, 73. (e) Fujitsuka, M.; Masuhara, A.; Kasai, H.; Oikawa, H.; Nakanishi, H.; Ito, O.; Yamashiro, T.; Aso, Y.; Otsubo, T. *J. Phys. Chem. B* **2001**, *105*, 9930.

(17) (a) van Hal, P. A.; Knol, J.; Langeveld-Voss, B. M. W.; Meskers, S. C. J.; Hummelen, J. C.; Janssen, R. A. J. *J. Phys. Chem. A* **2000**, *104*, 5974. (b) Beckers, E. H. A.; van Hal, P. A.; Dhanabalan, A.; Meskers, S. C. J.; Knol, J.; Hummelen, J. C.; Janssen, R. A. J. *J. Phys. Chem. A* **2003**, *107*, 6218.

(18) (a) Arbogast, J. W.; Foote, C. S.; Kao, M. *J. Am. Chem. Soc.* **1992**, *114*, 2277. (b) Foote, C. S. *Top. Curr. Chem.* **1994**, *169*, 347.

(19) Wang, Y. *J. Phys. Chem.* **1992**, *96*, 764.

(20) (a) Seshadri, R.; Rao, C. N. R.; Pal, H.; Mukherjee, T.; Mittal, J. P. *Chem. Phys. Lett.* **1993**, *205*, 395. (b) Ghosh, H. N.; Pal, H.; Saper, A. V.; Mittal, J. P. *J. Am. Chem. Soc.* **1993**, *115*, 11722.

(21) Schaffner, E.; Fischer, H. *J. Phys. Chem.* **1993**, *97*, 13149.

(22) (a) Watanabe, A.; Ito, O. *J. Phys. Chem.* **1994**, *98*, 7736. (b) Ito, O.; Sasaki, Y.; Yoshikawa, Y.; Watanabe, A. *J. Phys. Chem.* **1995**, *99*, 9838. (c) Alam, M. M.; Watanabe, A.; Ito, O. *J. Photochem. Photobiol., A* **1997**, *104*, 59. (d) Luo, C.; Fujitsuka, M.; Watanabe, A.; Ito, O.; Gan, L.; Huang, Y.; Huang, C. H. *J. Chem. Soc., Faraday Trans.* **1998**, *94*, 527. (e) Sandanayaka A. S. D.; Araki, Y.; Luo, C.; Fujitsuka, M.; Ito, O. *Bull. Chem. Soc. Jpn.* **2004**, *77*, 1313.

(23) Wienk, M. M.; Janssen, R. A. J. *Chem. Commun.* **1996**, 267.

(24) (a) Stickley, K. R.; Selby, T. D.; Blackstock, S. C. *J. Org. Chem.* **1997**, *62*, 448. (b) Ishikawa, M.; Kawai, M.; Ohsawa, Y. *Synth. Met.* **1995**, *40*, 231.

(25) Komamine, S.; Fujitsuka, M.; Ito, O.; Morikawa, K.; Miyata, T.; Ohno, T. *J. Phys. Chem. A* **2000**, *104*, 11497.

(26) Rajkumar,G. A.; Sandanayaka, A. S. D.; Ikeshita, K.; Itou, M.; Araki, Y.; Furusho, Y.; Kihara, N.; Ito, O.; Takata, T. *J. Phys. Chem. A* **2005**, *109*, 2428.

(27) (a) Boulle, C.; Rabreau, J. M.; Hudhomme, P.; Cariou, M.; Jubault, M.; Gorgues, A.; Orduna, J.; Garín, J. *Tetrahedron Lett.* **1997**, *38*, 3909. (b) Kreher, D.; Hudhomme, P.; Gorgues, A.; Luo, H.; Araki, Y.; Ito, O. *Phys. Chem. Chem. Phys.* **2003**, *5*, 4583.

(28) Guo, X.; Gan, Z.; Luo, H.; Araki, Y.; Zhang, D.; Zhu, D.; Ito, O. *J. Phys. Chem. A* **2003**, *107*, 9747.

(29) (a) Allard, E.; Delaunay, J.; Cheng, F.; Cousseau, J.; Ordúna, J.; Garín, J. *Org. Lett.* **2001**, *3*, 3503. (b) Allard, E.; Cousseau, J.; Ordúna, J.; Garín, J.; Luo, H.; Araki, Y.; Ito, O. *Phys. Chem. Chem. Phys.* **2002**, *4*, 5944.

(30) Watanabe, N.; Kihara, N.; Takata, T. *Org. Lett.* **2001**, *3*, 3519.

(31) (a) Watanabe, N.; Kihara, N.; Furusho, Y.; Takata, T.; Araki, Y.; Ito, O. *Angew. Chem., Int. Ed.* **2003**, *42*, 681. (b) Sandanayaka, A. S. D.; Watanabe, N.; Ikeshita, K.; Araki, Y.; Kihara, N.; Furusho, Y.; Ito, O.; Takata, T. *J. Phys. Chem. B* **2005**, *109*, 2516.

(32) Weller, A. *Z. Phys. Chem. Neue Folge* **1982**, *133*, 93.

(33) (a) Ma, B.; Lawson, G. E.; Bunker, C. E.; Kitaygorodskiy, A.; Sun, Y.-P. *Chem. Phys. Lett.* **1995**, *247*, 51. (b) Sun, Y.-P.; Ma, B.; Lawson, G. E. *Chem. Phys. Lett.* **1995**, *233*, 57. (c) Lawson, G. E.; Kitaygorodskiy, A.; Ma, B.; Bunker, C. E.; Sun, Y.-P. *J. Chem. Soc., Chem. Commun.* **1995**, 2225.

(34) (a) Marcus, R. A. *J. Chem. Phys.* **1956**, *24*, 966. (b) Marcus, R. A. *J. Chem. Phys.* **1965**, *43*, 679. (c) Marcus, R. A.; Sutin, N. *Biochim. Biophys. Acta* **1985**, *811*, 265.

(35) (a) Sandanayaka, A. S. D.; Sasabe, H.; Araki, Y.; Furusho, Y.; Ito, O.; Takata, T. *J. Phys. Chem. A* **2004**, *108*, 5145. (b) He-Ping, Z.; Wang, T.; Sandanayaka, A. S. D.; Araki, Y.; Ito, O. *J. Phys. Chem. A* **2005**, *109*, 4713.

(36) Yamanaka, K.; Fujitsuka, M.; Araki, Y.; Ito, O.; Aoshima, T.: Fukushima, T.; Miyashi, T. *J. Phys. Chem. A* **2004**, *108*, 250.

(37) Luo, H.; Fujitsuka, M.; Araki, Y.; Ito, O.; Padmawar, P.; Chiang, L. Y. *J. Phys. Chem. B* **2003**, *107*, 9312.

(38) (a) Yamazaki, M.; Araki, Y.; Fujitsuka, M.; Ito, O. *J. Phys. Chem. A* **2001**, *105*, 8615. (b) D'Souza, F.; Deviprasad, G. R.; Zandler, M. E.; Hoang, V. T.; Klykov, A.; El-Khouly, M. E.; Fujitsuka, M.; Ito, O. *J. Phys. Chem. B* **2002**, *106*, 4952.